# Chain-End Functionalized Nanopatterned Polymer Brushes Grown *via in Situ* Nitroxide Free Radical Exchange

**Sarav B. Jhaveri,[†] Matthias Beinhoff,[‡] Craig J. Hawker,[§] Kenneth R. Carter,[∥,*] and Dotsevi Y. Sogah[†,*]**

[†]Baker Laboratory, Department of Chemistry and Chemical Biology, Cornell University, Ithaca, New York 14853, [‡]Center for Polymeric Interfaces and Macromolecular Assemblies at IBM Almaden Research Center, San Jose, California 95120, [§]Materials Research Laboratory, University of California, Santa Barbara, California 93106, and [∥]Polymer Science and Engineering Department, University of Massachusetts-Amherst, Conte Center for Polymer Research, 120 Governors Drive, Amherst, Massachusetts 01003

**ABSTRACT** The patterning of biologically active materials has been accomplished by the use of imprint lithography of functional photopolymer resins to create controlled nanoscale patterns of a cross-linked photopolymer containing embedded initiator groups. Functionalized polymer brushes consisting of polystyrene and poly(*N*,*N*-dimethylacrylamide) were grown from these patterned layers by nitroxide-mediated polymerization. Chain-end functionalization of the brush layer was accomplished by nitroxide radical exchange during the polymerization. Accordingly, brush layers terminated by pyrene and biotin functional groups were obtained by exchange with the appropriate alkoxyamines. The presence of pyrene functionality at the chain ends of the brushes was confirmed by fluorescent emission measurements. Fluorescently labeled streptavidin protein was selectively attached with high selectivity to the patterned biotinylated brush layer through biotin—streptavidin interactions. The functionalized polymer grafted surfaces and nanopatterns have been successfully characterized using a fluorescence spectrophotometer, AFM, SEM, confocal microscopy, and water contact angle measurements.

The arbitrary patterning of biomolecules such as proteins and peptides on surfaces is useful for the development of cellular biosensors, biomaterials, and genomic arrays.[1,2] Biorecognition occurs over many length scales, and some of the most important events take place at the molecular or nanometer level; hence, robust and modular routes toward fabricating arrays with such precision become necessary.[3] Reports on a number of methods for preparing arrays approaching such precision have been described, including conventional photolithography, scanning probe techniques, nanografting, dip-pen nanolithography, contact lithography, printing, and self-assembled monolayers. A comprehensive review covering these and other methods has recently appeared.[4]

Of the many patterning techniques being pursued, contact lithographic processes, such as nanoimprint lithography, show great promise.[5,6] Imprint techniques have the advantage that they are not serial processes; hence, large areas can be simultaneously patterned with features of different length scales. Additionally, imprint equipment is not as complex or costly as other advanced patterning tools, allowing for high throughput, low cost fabrication.[7] Patterning of proteins on surfaces has been accomplished by thermal nanoimprint lithography (NIL) to produce patterned active layers.[8–10] In each of these cases, the first step is the imprinting of a poly(methylmethacrylate) (PMMA) layer that had been applied to a silicon wafer surface. After patterning of the PMMA, standard lithographic techniques such as masked deposition or inert material deposition followed by lift-off, and additional application of active materials, patterned layers of active materials on the silicon wafer surface were created. These active layers are either self-assembled

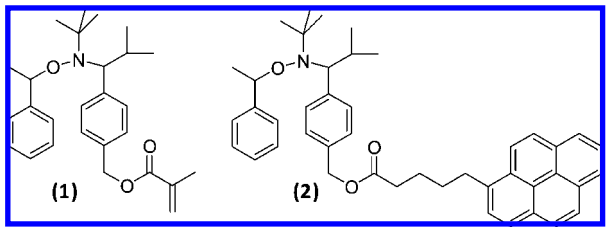


**Figure 1. Structure of inimer (1) containing both a methacrylate group for incorporation into the photopolymer and an alkoxyamine group for subsequent brush growth. Structure of pyrene-functionalized alkoxyamine initiator (2) used in nitroxide exchange reactions.**

*Address correspondence to krcarter@polysci.umass.edu.

Received for review January 7, 2008 and accepted March 03, 2008.

**Published online April 2, 2008.**
10.1021/nn8000092 CCC: $40.75

© 2008 American Chemical Society

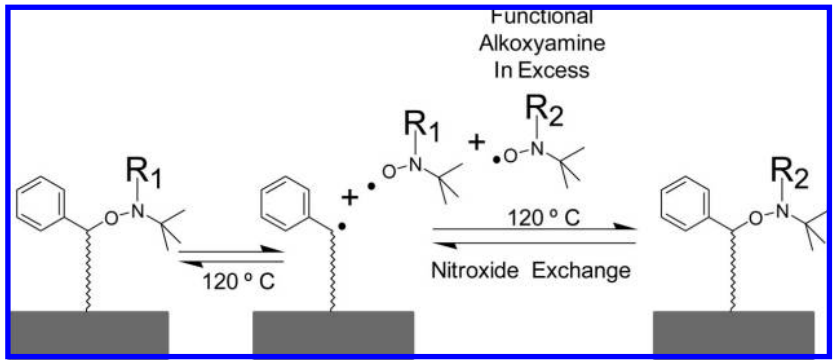


**Figure 2. Nitroxide exchange principle describing the transfer of functional groups at chain ends of polymer brushes during surface-initiated NMP.**

monolayers (SAMs)[9,10] or adsorbed copolymers[8] which permit patterning of proteins in the sub-100 nm size range.

Another imprint method that has shown utility in the patterning of functional materials is nanocontact molding (NCM).[11,12] An advantage of this technique compared with other available imprint methods is precise control of the chemistry through surface modification and incorporation of reactive functionality into the patterned cross-linked polymers. Complex functionality can be obtained by the covalent incorporation of functional inimers (compounds having both an **ini**tiator and mono**mer** fragments) for "living" free radical polymerization into the photopolymer matrix (sample inimer structure is shown in Figure 1). Controlled "living" radical secondary brush polymerizations of styrene, acrylates, and other vinyl monomers from the embedded inimer sites yield polymer brush surfaces that offer the capability for adjusting imprinted feature sizes and chemical functionalities in the nanometer-size regime.[13] As a result, the surface properties of the patterned substrate can be radically altered. The grafting density of these brushes is quite high though difficult to determine due to the uncertainty in quantifying the accessibility of embedded inimer groups. Previous studies have shown that brush growth from films with inimer concentration as low as 5% gave brush height and molecular weight profiles consistent with densely packed brush layers. Patterned layers of polyflurorene grafts have also been made by an extension of this technique.[14] In a recent report, the utility of the patterning of polymers with embedded functionality to create metallic nanostructures has been described.[15]

This current paper concerns a careful examination of the use of NCM to pattern a functional resin that is subsequently converted into a scaffold for the selective recognition and attachment of streptavidin protein. In the approach used here, NCM is performed on a photopolymer composition containing an alkoxyamine-based inimer. After patterning, brushes consisting of poly(*N*,*N*-dimethylacrylamide) (PDMA) are grown from the patterned layer by nitroxide-mediated polymerization (NMP).[16,17] The key enabling step here is a new and robust technique for introducing functional groups at chain ends of surface-grafted polymer brushes *via* an *in situ* functionalized nitroxide radical exchange process, which occurs during the surface-initiated polymerization reaction. Though such nitroxide exchange has been described for linear polymers synthesized in solution,[18,19] the use of this radical crossover chemistry from surface-grafted brushes has not been reported. This selective functionalization of the brush layer by alkoxyamine exchange occurs in a process whereby an alkoxyamine containing the desired functionality is exchanged with the inimer alkoxyamine during brush growth

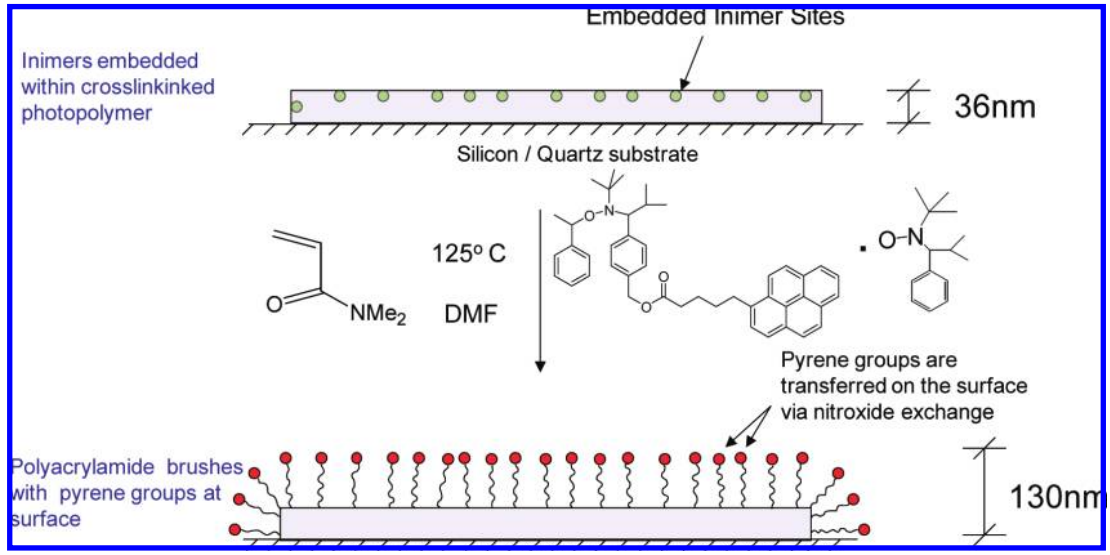


**Figure 3. Polymer brush growth concurrent with nitroxide exchange leading to PDMA brush layers end-capped with pyrene-functionalized alkoxyamine.**

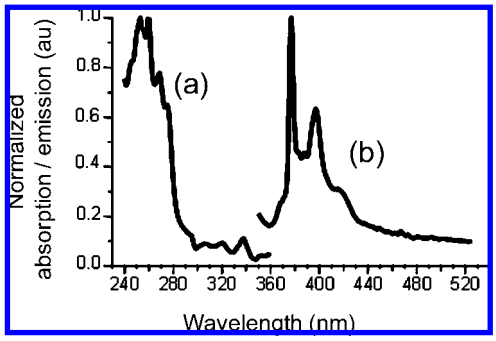


**Figure 4. Absorbance (a) and emission (b) spectra of pyrene chain-end functionalized PDMA brushes.**

in such a way that, by the end of brush growth, the majority of brush chains are terminated with the functionalized nitroxide. Under the proper reaction conditions, this exchange process has been shown to be both rapid and quantitative, while at below 80 °C, the alkoxyamine chain end has been shown in numerous studies to be fully stable.[18] The nitroxide exchange process is illustrated in Figure 2 where end functionality $R_1$ is replaced by $R_2$. Using this functionalized nitroxide radical exchange process, pyrene and biotin functionalities have been incorporated at the chain ends of patterned PDMA brushes grown *via* surface-initiated NMP. The biotin chain-end functionalities on the nanopatterned surfaces have been utilized as selective binding sites for streptavidin protein, resulting in the surface patterning of proteins. These systems also demonstrate a significant feature of this technique in that it opens up access to a wide array of functionalized structures and permits the incorporation of functional groups that are either very costly or incompatible with other patterning procedures. The modular nature of the process also allows libraries of functionalized structures to be prepared from one base material.

## RESULTS AND DISCUSSION

To demonstrate the effective use of nitroxide exchange to introduce surface-tethered functional groups during surface-initiated polymerization, a pyrene-functionalized alkoxyamine initiator, **2** (shown in Figure 1), was prepared[20] as an agent to transfer pyrene groups to the chain ends of nanopatterned PDMA brushes. PDMA was selected due to its hydrophilicity and biocompatibility, hence its great potential in pharmaceutical and biomedical applications.[21–23] Studies have demonstrated that surfaces grafted with polymers such as PDMA and polyethylene glycol (PEG) minimize protein adsorption as compared with hydrophobic or other polar surfaces.[24–26] While living free radical polymerization of *N*,*N*-dimethylacrylamide is challenging, reports of controlled preparation of PDMA with low polydispersities have appeared. These include NMP,[27–30] atom transfer radical polymerization (ATRP),[31–34] and reversible addition−fragmentation chain transfer (RAFT).[35,36]

Initial experiments to test the nitroxide exchange principle were performed from flat polymer films. Accordingly, the inimer containing methacrylate-based photopolymer was applied to a silicon wafer surface by spin-coating and cured under UV light (365 nm). It should be noted that this wavelength is absorbed by pyrene units, so the presence of **2** in the original photopolymer mixture leads to inefficient cross-linking and thus prevents network formation. However, this is not the case for the secondary thermal process where PDMA brushes were grown from the cured photopolymer surface by NMP performed in the presence of an

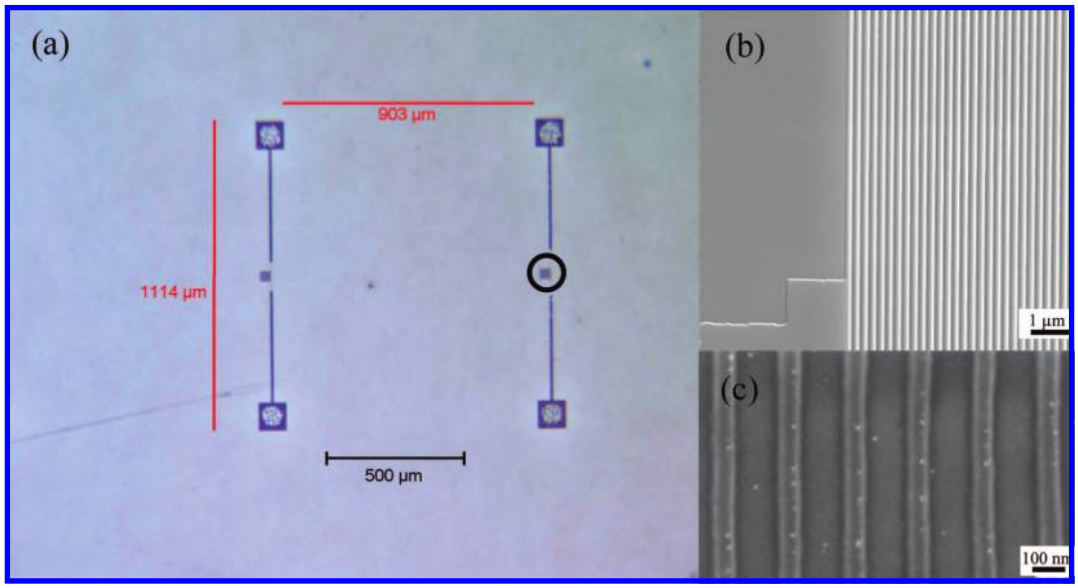


**Figure 5. Images (a) and (b) show the patterned silicon master where (a) is an optical microscope image and image (b) is the SEM image of the highlighted circular region in image (a), showing 75 nm line patterns. Image (c) is the SEM image of the polymer layer after nanocontact molding with the 75 nm lines region shown.**

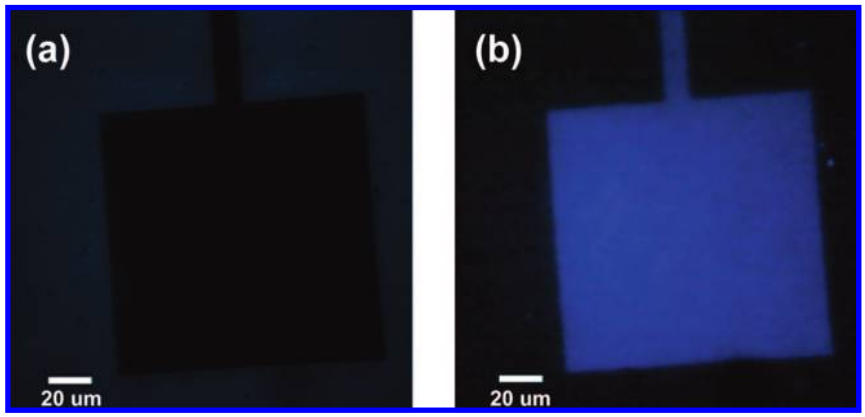


**Figure 6. Optical microscope fluorescence images of pyrene functionalized patterned PS brushes. (a) When exposed at excitation wavelengths ($\lambda_{exc}$) between 450 and 490 nm, no fluorescence is observed. (b) When illuminated at $\lambda_{exc}$ 330–380 nm, bright fluorescence is observed from the pyrene groups at chain ends of the PS brushes.**

excess of alkoxyamine **2**, leading to nitroxide exchange during polymerization (Figure 3). After polymerization, the wafer was removed from the reaction vessel and washed extensively with acetone, dichloromethane, THF, and water to ensure complete removal of any free polymer from the wafer surface. Brush growth was confirmed by ellipsometry, as the film's thickness after brush growth increased from 36 to 130 nm. Brush growth was further supported by water contact angle measurements where the contact angle decreased from 81° (before polymerization) to 54° (after polymerization). The presence of pyrene end-groups was confirmed by UV/vis absorption and fluorescence measurements, where the functionalized surface had the expected pyrene absorbance peak at 335 nm and fluorescence emission peaks at 375 and 405 nm (excitation wavelength of 330–380 nm) (Figure 4).

One consequence of performing brush growth by NMP while using an excess of alkoxyamine is the formation of "free" polymer chains in solution concurrent with surface brush growth.[13] This free polymer was precipitated and analyzed by gel permeation chromatography (GPC) in order to estimate the molecular weight and polydispersity of the PDMA brushes which were found to be $M_n$ = 24 000 and PDI = 1.18 demonstrating the controlled nature of the growth process and the potential to tune the thickness of the resulting thin films.[37] The brushes grown from these surfaces are consistent with what would be expected for densely packed brush layers, not low-density mushroom-like grafting coverage.

Nanocontact molding was used to prepare patterns of the inimer embedded photopolymer in a manner similar to previously reported studies.[13,15,38] Molds containing arbitrary test patterns with features ranging from 100 nm to 10 μm were used. An optical micrograph image of the original silicon used in the nanocontact molding process is shown in Figures 5a, and a close-up of the 75 nm wide lines is shown in Figure 5b (SEM). The patterned inimer embedded photopolymer replica is shown in Figure 5c. Clearly, the nanocontact molding process very accurately reproduced the 75 nm line features of the master.

Surface NMP of styrene in the presence of excess alkoxyamine, **2**, was utilized to grow pyrene-functionalized polystyrene (PS) brushes from these patterned photopolymer features. The fluorescence emitted from the chain ends of the patterned PS brushes was clearly visible by optical microscopy (Figure 6). The emission of fluorescence was only observed when exposed in the range of 330–380 nm, and the patterns did not fluoresce when exposed to other wavelengths. A closer examination of the patterned surfaces was performed by atomic force microscopy (AFM) (Figure 7) and scanning electron microscopy (SEM) (Figure 8). The patterned pyrene-functionalized PS brushes show an increase in the width of the patterned lines. The initial feature width of the initiator embedded line was 75 nm which increased to 111 nm (Δ 36 nm) after the PS brush growth. Brush growth was further supported by water contact angle measurements where the contact angle increased from 81° (before polymerization) to 96° (after polymerization). GPC of the free PS polymer isolated from the reaction solution had $M_n$ = 34 700 and PDI = 1.16. The success of this procedure demonstrates the ability to control the feature size, surface properties, and functionality of nanoscale features.

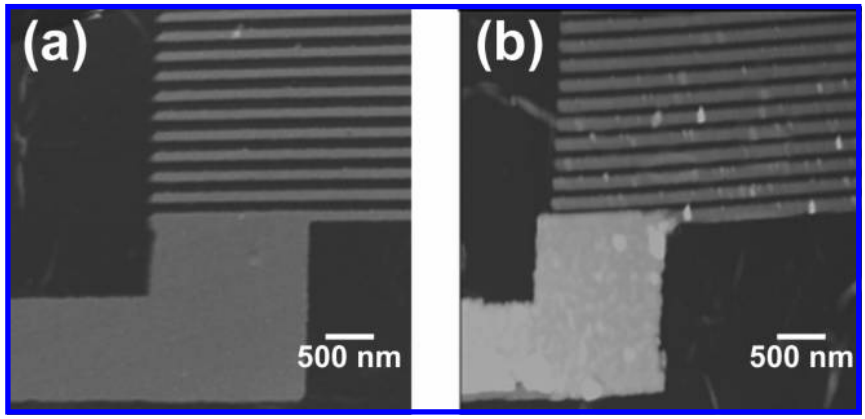


**Figure 7. AFM plots of the (a) inimer embedded patterned lines before polymerization and (b) after polymerization of pyrene-functionalized PS brushes (*z* range = 100 nm).**

The complex of biotin with streptavidin and its structural homologue avidin are known to be among the strongest ligand−protein complexes,[39] with measured binding constants of 1.7 ×

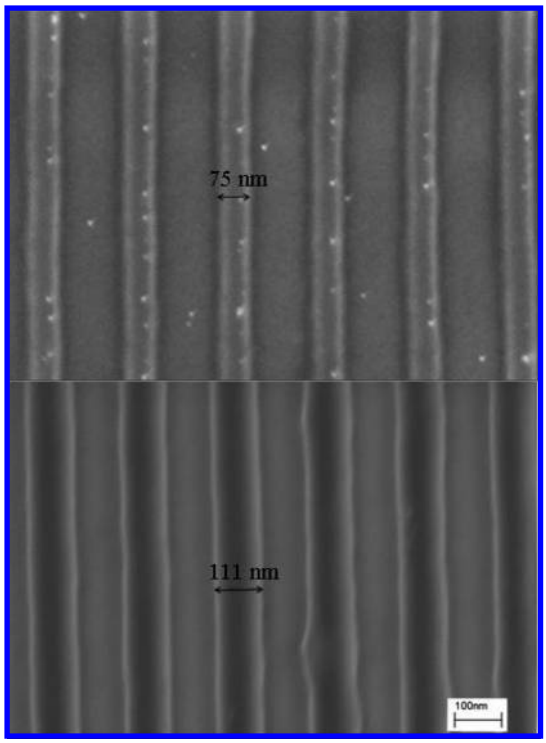


**Figure 8. SEM images of the patterned lines before (top) and after (bottom) polymerization of pyrene-functionalized PS brushes.**

$10^{15}$ and $2.5 \times 10^{13}$, respectively.[39,40] Because of the very high binding affinities of biotin to these two proteins, biotin−streptavidin systems have been used effectively for attachment of streptavidin to biotinylated polymers,[41–47] carbon nanotubes,[48] *etc.* Additionally, since streptavidin is a tetramer with four binding sites, each site binding to one molecule of biotin, it has been shown that surface engineering of various other biotinylated proteins on streptavidin-bound surfaces is possible.[44,47,49–51]

An alkoxyamine initiator bearing biotin was synthesized for the preparation of patterned brush layers end-capped with biotin functionality for the selective attachment of streptavidin protein. Hydroxymethyl-functionalized alkoxyamine, **3**, was chosen as the precursor for the functionalization scheme (Figure 9). The alcohol group of the starting alkoxyamine was converted to the bromo group using carbon tetrabromide ($CBr_4$) and triphenyl phosphine ($PPh_3$) to afford the bromide-functionalized alkoxyamine, **4**, in almost quantitative yield. The bromide functional alkoxyamine, **4**, was converted to the azide, **5**, using sodium azide ($NaN_3$) in 71% yield. This was subsequently reduced using $LiAlH_4$ to give the amine-functionalized alkoxyamine, **6**, in 92% yield, which was reacted with an activated biotin-functionalized ester (biotin-*N*-hydroxysuccinimide ester, **7**) in the presence of triethylamine to produce the biotin-functionalized alkoxyamine initiator, **8**. The biotinylated alkoxyamine was used in the nitroxide exchange during NMP of dimethylacrylamide from the patterned inimer embedded photopolymer yielding PDMA brush layers with biotinylated end-groups. SEM images (Figure 10) taken before and after the growth of the patterned brushes showed an increase in the height of the patterned lines. The initial width of the initiator embedded line was 75 nm which increased to 114 nm (Δ 39 nm) after brush polymerization. As described for the pyrene reactions above, the free solution PDMA was isolated and analyzed and found to have an $M_n = 8750$ and PDI = 1.16.

A substrate with the patterned biotinylated PDMA brushes was immersed in a HEPES buffered saline solution of fluorescently tagged Alexa-488 streptavidin (0.1 μM) for 45 min. The substrate was removed from the solution, washed with excess buffer solution, and dried in air. Selective binding of fluorescently tagged Alexa-488 streptavidin was observed on the biotin-functionalized brush patterns using confocal microscopy (Figure 11). As a control, PDMA brushes were grown using alkoxyamine, **10**, that did not have biotin functionality. These substrates were also allowed to react with fluorescently tagged Alexa-488 streptavidin as described above. After being rinsed and dried, these PDMA brush layers showed no observable attachment of streptavidin. For the biotinylated brushes, the contrast between the patterned areas and the underlying silicon substrate showed the high selectivity of the attachment to the brush layer and the relatively low level of nonspecific adsorption of protein on the silicon surface.

## CONCLUSIONS

We have successfully demonstrated that *in situ* nitroxide radical exchange during NMP is a simple and effective technique for introduction of functionality

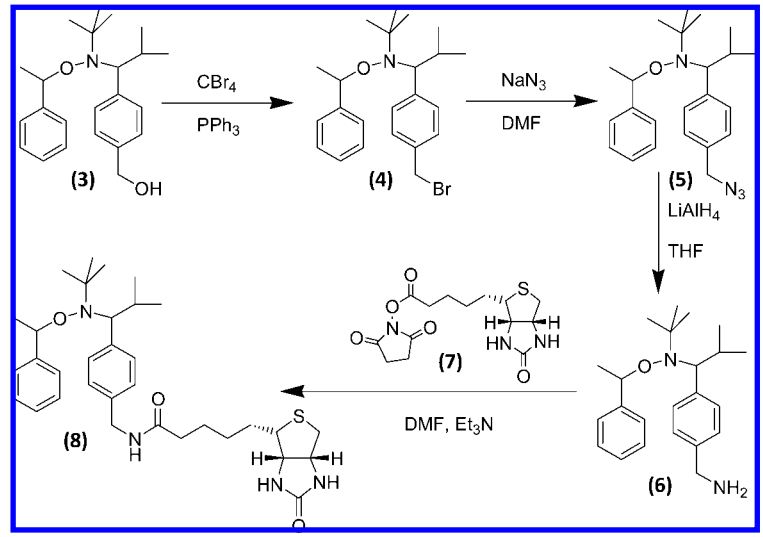


**Figure 9. Synthesis of biotin-functionalized alkoxyamine 8.**

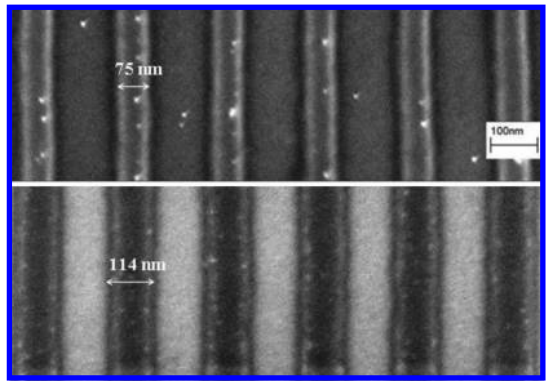


**Figure 10. SEM images of inimer embedded photopolymer (top) and biotinylated PDMA brushes after nitroxide exchange reaction (bottom).**

to chain ends of grafted polymer layers. Pyrene and biotin functional groups have been successfully incorporated at the chain end of patterned polymer brush layers with the polymer grafted surfaces and nanopatterns characterized by fluorescence measurements, AFM, SEM, confocal microscopy, and water contact angle measurements. The MW of the free polymer grown concurrently in solution was used to approximate the molecular weight of the bushes. The results demonstrate accurate control over feature size and polymer brush thickness. The patterned biotinylated polymer brush layers have been utilized in the specific binding of streptavidin protein. Since streptavidin has a tetrahedral symmetry with four binding sites for biotin, further studies are presently being conducted to attach biotinylated nanoparticles and protein sequences on these nanopatterned streptavidin-functionalized surfaces. We

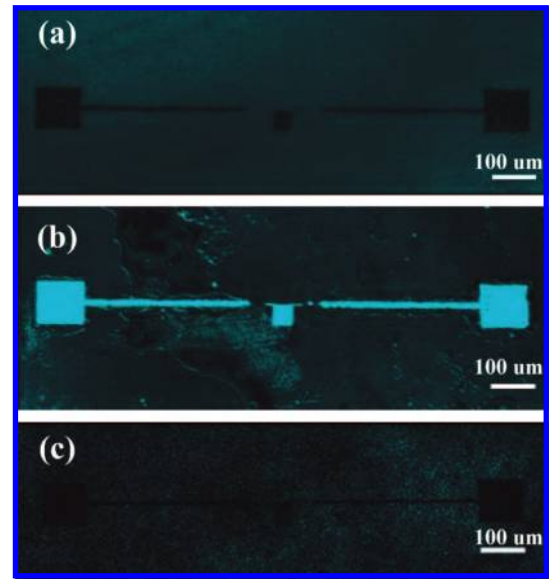


**Figure 11. Confocal microscope images of (a) biotin-functionalized patterned PDMA brushes, (b) patterned PDMA brushes incubated in Alexa 488 labeled streptavidin, and (c) unfunctionalized PDMA brushes incubated in Alexa 488 labeled streptavidin. Scale bar = 100 μm.**

believe the described method of polymer brush functionalization using a functionalized radical exchange process during surface-initiated living free radical polymerization is a robust and modular tool to control both the dimensions and the functionality of grafted polymer brushes on the nanometer scale. The ability to pattern biologically relevant materials at this length scale with the ease and speed demonstrated will enable new device and sensor development.

## METHODS

**Materials.** All chemical reactions were performed under $N_2$ unless noted. THF was distilled under $N_2$ from sodium benzophenone. DMF was used as received. Styrene was freshly distilled from $CaH_2$ prior to use. *N*,*N*-dimethyl acrylamide was passed through a basic alumina column prior to use. All chemicals were purchased from Sigma Aldrich and unless noted were used as received. Streptavidin, Alexa Fluor 488 conjugated/tagged, was purchased from Molecular Probes (Invitrogen). Syntheses of inimer (**1**),[13] pyrene-functionalized alkoxyamine (**2**),[20] hydroxymethyl-functionalized alkoxyamines (**3**),[20] biotin-*N*-hydroxy succinimide ester (**7**),[52] 2,2,5-trimethyl-4-phenyl-3-azahexane-3-nitroxide (TIPNO, **9**),[27] and 2,5-dimethyl-3-(1-phenylethoxy)-4-phenyl-3-azahexane (**10**)[27] were performed in accordance with literature procedures. The alkoxyamine initiator embedded patterns were prepared as previously described in the literature,[13] using a nanocontact molding process and a methacrylate-based photocurable resin.

**Characterization.** Nuclear magnetic resonance (NMR) spectroscopy was performed on a Varian Unity 400 MHz NMR spectrometer using deuterated chloroform ($CDCl_3$) as solvent and the internal solvent peak as the reference. Electrospray mass spectroscopy (ESMS) was taken at Cornell BioResource Center using a Bruker Esquire-LC ion trap mass spectrometer. GPC was carried out on a Waters chromatograph (four Waters Styragel HR columns HR1, HR2, HR4, and HR5E in series) connected to a Waters 410 differential refractometer with THF as the carrier solvent. The SEM images were taken using a LEO 1550 SEM with a Schottky field emission source. The confocal microscopy was performed using a Leica TCS SP2 scanning confocal microscope. UV/vis absorption spectra were recorded using an HP 8452A diode array spectrometer. Emission was measured using an SA Instruments FL3-11 fluorimeter. Epifluorescent microscopy was performed using a Nikon E400 microscope body equipped with a Nikon EPI EF illumination unit and a 100 W mercury light source. AFM images of polymer patterns were obtained with a Digital Instruments Dimension 5000 in intermittent contact mode at a scan rate of 1 Hz. Samples were imaged under ambient conditions with silicon nitride cantilevers (spring constant 0.58 N/m).

**Synthesis of Bromine-Functionalized Alkoxyamine (4).** To a solution of alkoxyamine alcohol **3** (2.01 g, 5.65 mmol) in THF (10 mL) was added $CBr_4$ (2.33 g, 7.03 mmol) followed by portionwise addition of $PPh_3$ (1.84 g, 7.03 mmol). The reaction was quenched after 5 min with 2 mL of water. The reaction mixture was concentrated using a rotatory evaporator. Dichloromethane and water (50 mL each) were added. The organic layer was removed and dried over $MgSO_4$, filtered, and evaporated to dryness. The crude product was purified by flash chromatography, starting with pure hexanes and increasing to 1:1 hexanes/$CH_2Cl_2$ to obtain 2.36 g (99%) of bromide, **4**, as a colorless oil.

$^1$H NMR (400 MHz, $CDCl_3$, both diastereomers) δ 7.4–7.1 (m, 18H), 4.90 (q + q, 2H, $J$ = 6.5 Hz, both diastereomers), 4.48 and 4.45 (each s, 4H, $CH_2Cl$), 3.41 (d, 1H, $J$ = 10.4 Hz, major diastereomer), 3.29 (d, 1H, $J$ = 10.8 Hz, minor diastereomer), 2.30 (two

m, 2H, both diastereomers), 1.61 (d, 3H, $J$ = 6.4 Hz, major diastereomer), 1.53 (d, 3H, $J$ = 6.4 Hz, minor diastereomer), 1.30 (d, 3H, $J$ = 6.4 Hz, major diastereomer), 1.03 (s, 9H, major diastereomer), 0.91 (d, 3H, $J$ = 6.4 Hz, minor diastereomer), 0.76 (s, 9H, minor diastereomer), 0.52 (d, 3H, $J$ = 6.8 Hz, major diastereomer), and 0.20 (d, 3H, $J$ = 6.8 Hz, minor diastereomer). $^{13}$C NMR (100 MHz, $CDCl_3$, both diastereomers) δ 145.8 (d), 143.276 (d), 143.071 (d), 135.952 (d), 135.741 (d), 131.446–126.377 aromatic region, 83.766 (d), 83.187 (d), 72.000 (d), 71.874 (d), 60.774 (d), 60.615 (d), 32.204 (d), 31.784 (d), 28.651 (t), 28.585 (t), 28.460 (t), 24.889 (s), 23.312 (s), 22.321 (d), 22.154 (d), 21.395 (d), 21.264 (d). ESI MS [M + 1 peak] calcd 419.41, obsd 420.20. HRMS calcd for $C_{23}H_{32}BrNO$ 417.166725, found 417.1662. Elemental Analysis: Calcd C, 66.02; H, 7.70; N, 3.34. Found: C, 65.38; H, 7.64; N, 3.09.

**Synthesis of Azide-Functionalized Alkoxyamine (5).** A mixture of **4** (2.36 g, 5.66 mmol), sodium azide (1.11 g, 17 mmol), and 18-crown-6 (25 mg) was stirred in DMF (15 mL) at 60 °C for 16 h. The reaction mixture was then poured into water (150 mL) and extracted with $CH_2Cl_2$ (3 × 40 mL). The organic fractions were dried with $MgSO_4$, filtered, and evaporated to dryness. The residue was purified by flash column chromatography eluting with 1:1 petroleum ether/$CH_2Cl_2$ to obtain 1.53 g (71%) of azide-functionalized alkoxyamine, **5**, as a light yellow oil.

$^1$H NMR (400 MHz, $CDCl_3$, both diastereomers) δ 7.45–7.11 (m, 18H), 4.91 (q + q, 2H, $J$ = 3.6 Hz, both diastereomers), 4.33 and 4.27 (each s, 4H, $CH_2N_3$, major and minor diastereomers), 3.44 (d, 1H, $J$ = 10.8 Hz, major diastereomer), 3.32 (d, 1H, $J$ = 10.4 Hz, minor diastereomer), 2.34 (two m, 2H, both diastereomers), 1.63 (d, 3H, $J$ = 6.8 Hz, major diastereomer), 1.55 (d, 3H, $J$ = 6.4 Hz, minor diastereomer), 1.32 (d, 3H, $J$ = 6.8 Hz, major diastereomer), 1.05 (s, 9H, major diastereomer), 0.93 (d, 3H, $J$ = 6.4 Hz, minor diastereomer), 0.78 (s, 9H, minor diastereomer), 0.55 (d, 3H, $J$ = 6.4 Hz, major diastereomer), and 0.22 (d, 3H, $J$ = 6.8 Hz, minor diastereomer). $^{13}$C NMR (100 MHz, $CDCl_3$, both diastereomers) δ 145.857 (d), 145.080 (d), 143.011 (d), 142.793 (d), 133.388 (d), 133.182 (d), 131.540–126.379 aromatic region, 83.762 (d), 83.127 (d), 72.058 (d), 71.948 (d), 60.761 (s), 60.623 (s), 54.902 (d), 54.873 (d), 28.695 (t), 28.634 (t), 28.445 (t), 24.912(s), 23.353 (s), 22.337 (s), 22.168 (s), 21.365 (s), 21.237 (s). ESI MS [M + 1 peak] calcd 381.53, obsd 381.30. HRMS calcd for $C_{23}H_{32}N_4O$ 380.257611, found 380.2581. Elemental Analysis: Calcd C, 72.59; H, 8.47; N, 14.72. Found: C, 72.64; H, 8.28; N, 14.95.

**Synthesis of Amine-Functionalized Alkoxyamine (6).** $LiAlH_4$ (148 mg, 4.02 mmol) was added slowly to **5** (1.53 g, 4.02 mmol) dissolved in THF (25 mL) and cooled to 0 °C. After the reaction was stirred under argon for 16 h, water (160 μL) was slowly added followed by filtration and concentration by a rotovaporator. The crude product was purified by flash column chromatography eluting with 5% MeOH/$CH_2Cl_2$ to obtain 1.31 g (92%) of amino-functionalized alkoxyamine, **6**, as a light yellow liquid.

$^1$H NMR (400 MHz, $CDCl_3$, both diastereomers) δ 7.41–7.06 (m, 18H), 4.88 (q + q, 2H, $J$ = 4.8 Hz, both diastereomers), 4.08 (s, 4H, both diastereomers), 3.39 (d, 1H, $J$ = 10.4 Hz, major diastereomer), 3.27 (d, 1H, $J$ = 10.4 Hz, minor diastereomer), 2.29 (two m, 2H, both diastereomers), 2.05 (s, 2H, both diastereomers), 1.87 (s, 2H, both diastereomers), 1.60 (d, 3H, $J$ = 6.4 Hz, major diastereomer), 1.51 (d, 3H, $J$ = 6.8 Hz, minor diastereomer), 1.28 (d, 3H, $J$ = 6.4 Hz, major diastereomer), 1.024 (s, 9H, major diastereomer), 0.90 (d, 3H, $J$ = 6.4 Hz, minor diastereomer), 0.752 (s, 9H, minor diastereomer), 0.51 (d, 3H, $J$ = 6.4 Hz, major diastereomer), and 0.19 (d, 3H, $J$ = 6.4 Hz, minor diastereomer). $^{13}$C NMR (100 MHz, $CDCl_3$, both diastereomers) δ 145.885 (d), 145.098 (d), 138.50 (d),131.263–126.225 aromatic region, 83.643 (d), 82.996 (d), 72.046 (d), 71.938 (d), 60.678 (s), 60.551 (s), 49.872 (s), 28.695 (t), 28.655 (t), 28.458 (t), 24.914 (s), 23.331 (s), 22.380 (d), 22.198 (d), 21.401 (d), 21.301 (d). ESI MS [M + 1 peak] calcd 355.53, obsd 355.40. HRMS calcd for $C_{23}H_{34}N_2O$ 354.267113, found 354.2647. Elemental Analysis: Calcd C, 77.92; H, 9.66; N, 7.90. Found: C, 78.18; H, 9.61; N, 7.75.

**Synthesis of Biotin-Functionalized Alkoxyamine (8).** To a solution of alkoxyamine **6** (0.49 g, 1.37 mmol) in DMF (8.8 mL) was added 1.76 mL of triethylamine. After the solution was stirred for 30 min, a solution of biotin-*N*-hydroxy succinimide ester **7** (0.47 g, 1.37 mmol) in DMF (3 mL) was added. The reaction mixture was stirred for 24 h at room temperature and then concentrated. The crude product was precipitated by addition of 100 mL of diethyl ether, filtered, and washed again with 50 mL of diethyl ether. NMR showed no presence of **7**. The product was further purified by flash column chromatography (2:8 $CH_3OH/CHCl_3$) to obtain 0.541 g (68%) of biotin-functionalized alkoxyamine, **8**, as a white solid. Melting point = 100–101 °C.

$^1$H NMR (400 MHz, $CDCl_3$, both diastereomers) δ 7.4–7.02 (m, 18H), 6.7(s, 2H, NH), 6.46 (bs, 2H, NH), 5.51 (s, 2H, NH), 4.85 (q + q, 2H, $J$ = 2.8 Hz, both diastereomers), 4.39–4.21 (s, 4H, $CH_2N$ and m,4H, NCHCHN), 3.36 (d, 1H, $J$ = 10.8 Hz, major diastereomer), 3.24 (d, 1H, $J$ = 10.8 Hz, minor diastereomer), 3.07 (bd, 2H, CHS, both diastereomers), 2.78 (m, 2H, CH2S), 2.61 (d, 2H, $J$= 12.8 Hz, CH2S), 2.21 (two m, 2H, both diastereomers), 2.20 (t, 4H, CH2, both diastereomers), 1.67 (bm,12H), 1.57 (d, 3H, $J$ = 6.4 Hz, major diastereomer), 1.50 (d, 3H, $J$ = 6.4 Hz, minor diastereomer), 1.25 (d, 3H, $J$ = 6.4 Hz, major diastereomer), 1.00 (s, 9H, major diastereomer), 0.87 (d, 3H, $J$ = 6.4 Hz, minor diastereomer), 0.73 (s, 9H, minor diastereomer), 0.47 (d, 3H, $J$ = 6.8 Hz, major diastereomer), and 0.14 (d, 3H, $J$ = 6.8 Hz, minor diastereomer). $^{13}$C NMR (100 MHz, $CDCl_3$, both diastereomers) δ 173.40 (s), 164.30 (s), 145.750 (d), 144.995 (d), 141.81 (d), 141.625 (d), 136.678 (d), 136.468 (d), 131.351–126.394 aromatic region, 83.635 (d), 83.077 (d), 71.926 (d), 71.810 (d), 61.933 (s), 60.704 (s), 60.565 (s), 60.359 (s), 43.359 (s), 40.667 (s), 36.313 (s), 32.243 (s), 31.864 (d), 31.837 (d), 28.633–21.276: aliphatic "C". ESI MS [M + 1 peak] calcd 581.83, obsd 581.30. HRMS calcd for $C_{33}H_{48}N_4O_3S$ 580.344713, found 580.3453. Elemental Analysis: Calcd C, 68.24; H, 8.33; N, 9.64. Found: C, 68.03; H, 8.45; N, 9.67.

**General Procedure for the Preparation of Chain-End Functionalized Polymer Brush Layers.** Silicon substrates covered with a patterned photopolymer that contained embedded initiators were prepared by nanocontact molding.[13] The substrates were immersed in a solution of DMF, monomer (styrene or *N,N*-dimethylacrylamide), and the desired alkoxyamine in a glass reaction vessel. Three freeze–pump–thaw cycles were applied before heating the reaction vessel to 125 °C under $N_2$ for 12 h. The reaction mixture was cooled and the polymerization solution decanted and added dropwise to methanol (in the case of polystyrene) or hexanes/diethylether (in the case of PDMA) to precipitate the polymer. The free polymer was filtered and dried. The silicon substrates were washed liberally with acetone, dichloromethane, THF, and water and then dried.

**Pyrene-Functionalized Patterned Polystyrene Brushes.** The general procedure above was followed with the use of pyrene-functionalized alkoxyamine **2** (24 mg, 3.84 μmol), styrene (2.5 mL, 2.27 g), and DMF (2.5 mL). The free polymer formed in solution was precipitated from methanol. Yield 1.31 g (58%). GPC molecular weight: $M_n$ 34 700 (calcd = 34 200); PDI = 1.16.

**Biotin-Functionalized Patterned PDMA Brushes.** The general procedure above was followed using the biotin-functionalized alkoxyamine **8** (24 mg, 41.32 μmol), *N,N*-dimethylacrylamide (1.50 g), DMF (2.5 mL), and 0.45 mg of free nitroxide (TIPNO, **9**). The free polymer formed in solution was precipitated from cold hexanes. Yield 0.35 g (23%). GPC molecular weight: $M_n$ = 8750 (calcd = 8470); PDI = 1.16.

**Binding of Streptavidin onto Biotin-Functionalized Nanopatterned Polymer Brushes.** Alexa 488 nm streptavidin solution (0.1 μM) was prepared using HEPES buffered saline (0.1 M NaCl; pH = 7.4) with 0.02% Tween 20 detergent (v/v) to prevent nonspecific binding. The silicon substrates containing patterned biotinylated polymer brush layers were immersed in 5 mL of 0.1 μM Alexa 488 nm streptavidin solution for 45 min. The wafers were removed, washed liberally with the buffer, and allowed to dry before being observed under a confocal microscope.

*Acknowledgment.* This work was supported in part by the Cornell Center for Materials Research (CCMR) with funding from the Materials Research Science and Engineering Center program of the National Science Foundation (cooperative agreement DMR-0079992), the STC Program of the National Science Foundation under Agreement No. ECS-9876771, the Chemical Biology Interface (CBI) Training Grant supported by the NIH, NSF, MRSEC Program Materials Research Laboratory, UC Santa Barbara (DMR-0520415), and the UMass Material Research Science and Engineering Center (MRSEC) (DMR-0213695). We also wish to

thank IBM for support. We would also like to acknowledge Malcolm Thomas for help with the SEM, Carol Bayles for confocal microscopy, Mark Hart for etching, Dr. Jane Frommer for AFM, Teddie Magbitang for GPC, and Kartikeya Pant for help on buffer preparation.

## REFERENCES AND NOTES


1. Irvine, D. J.; Doh, J.; Huang, B. Patterned Surfaces as Tools to Study Ligand Recognition and Synapse Formation by T Cells. *Curr. Opin. Immunol.* **2007**, *19*, 463–469.
2. Chen, C. S.; Mrksich, M.; Huang, S.; Whitesides, G. M.; Ingber, D. E. Geometric Control of Cell Life and Death. *Science* **1997**, *276*, 1425–1428.
3. Chen, G. Y. J.; Uttamchandani, M.; Lue, R. Y. P.; Lesaicherre, M. L.; Yao, S. Q. Array-Based Technologies and Their Applications in Proteomics. *Curr. Top. Med. Chem.* **2003**, *3*, 705–724.
4. Christman, K. L.; Enriquez-Rios, V. D.; Maynard, H. D. Nanopatterning Proteins and Peptides. *Soft Matter* **2006**, *2*, 928–939.
5. Chou, S. Y.; Krauss, P. R.; Renstrom, P. J. Imprint Lithography with 25-Nanometer Resolution. *Science* **1996**, *272*, 85–87.
6. Gates, B. D.; Xu, Q. B.; Stewart, M.; Ryan, D.; Willson, C. G.; Whitesides, G. M. New Approaches to Nanofabrication: Molding, Printing, and Other Techniques. *Chem. Rev.* **2005**, *105*, 1171–1196.
7. Bailey, T.; Choi, B. J.; Colburn, M.; Meissl, M.; Shaya, S.; Ekerdt, J. G.; Sreenivasan, S. V.; Willson, C. G. Step and Flash Imprint Lithography: Template Surface Treatment and Defect Analysis. *J. Vac. Sci. Technol., B.* **2000**, *18*, 3572.
8. Falconnet, D.; Pasqui, D.; Park, S.; Eckert, R.; Schift, H.; Gobrecht, J.; Barbucci, R.; Textor, M. A Novel Approach to Produce Protein Nanopatterns by Combining Nanoimprint Lithography and Molecular Self-Assembly. *Nano Lett.* **2004**, *4*, 1909–1914.
9. Hoff, J. D.; Cheng, L. J.; Meyhofer, E.; Guo, L. J.; Hunt, A. J. Nanoscale Protein Patterning by Imprint Lithography. *Nano Lett.* **2004**, *4*, 853–857.
10. Maury, P.; Escalante, M.; Peter, M.; Reinhoudt, D. N.; Subramaniam, V.; Huskens, J. Creating Nanopatterns of His-Tagged Proteins on Surfaces by Nanoimprint Lithography Using Specific Ninta-Histidine Interactions. *Small* **2007**, *3*, 1584–1592.
11. Mcclelland, G. M.; Hart, M. W.; Rettner, C. T.; Best, M. E.; Carter, K. R.; Terris, B. D. Nanoscale Patterning of Magnetic Islands by Imprint Lithography Using a Flexible Mold. *Appl. Phys. Lett.* **2002**, *81*, 1483–1485.
12. Mcclelland, G. M.; Rettner, C. T.; Hart, M. W.; Carter, K. R.; Sanchez, M. I.; Best, M. E.; Terris, B. D. Contact Mechanics of a Flexible Imprinter for Photocured Nanoimprint Lithography. *Tribol. Lett.* **2005**, *19*, 59–63.
13. Von Werne, T. A.; Germack, D. S.; Hagberg, E. C.; Sheares, V. V.; Hawker, C. J.; Carter, K. R. A Versatile Method for Tuning the Chemistry and Size of Nanoscopic Features by Living Free Radical Polymerization. *J. Am. Chem. Soc.* **2003**, *125*, 3831–3838.
14. Beinhoff, M.; Appapillai, A. T.; Underwood, L. D.; Frommer, J.; Carter, K. R. Patterned Polyfluorene Surfaces by Functionalization of Nanoimprinted Polymeric Features. *Langmuir* **2006**, *22*, 2411–2414.
15. Hagberg, E. C.; Scott, J. C.; Shaw, J. A.; Von Werne, T. A.; Maegerlein, J. A.; Carter, K. R. Mold and Metallization: Nanocontact Molding for the Fabrication of Metal Structures. *Small* **2007**, *3*, 1703–1706.
16. Hawker, C. J.; Bosman, A. W.; Harth, E. New Polymer Synthesis by Nitroxide Mediated Living Radical Polymerizations. *Chem. Rev.* **2001**, *101*, 3661–3688.
17. Husseman, M.; Malmstroem, E. E.; Mcnamara, M.; Mate, M.; Mecerreyes, D.; Benoit, D. G.; Hedrick, J. L.; Mansky, P.; Huang, E.; Russell, T. P.; Hawker, C. J. Controlled Synthesis of Polymer Brushes by "Living" Free Radical Polymerization Techniques. *Macromolecules* **1999**, *32*, 1424–1431.
18. Hawker, C. J.; Barclay, G. G.; Dao, J. Radical Crossover in Nitroxide Mediated "Living" Free Radical Polymerizations. *J. Am. Chem. Soc.* **1996**, *118*, 11467–11471.
19. Turro, N. J.; Lem, G.; Zavarine, I. S. A Living Free Radical Exchange Reaction for the Preparation of Photoactive End-Labeled Monodisperse Polymers. *Macromolecules* **2000**, *33*, 9782–9785.
20. Rodlert, M.; Harth, E.; Rees, I.; Hawker, C. J. End-Group Fidelity in Nitroxide-Mediated Living Free-Radical Polymerizations. *J. Polym. Sci. Part A, Polym. Chem.* **2000**, *38*, 4749–4763.
21. Harimoto, M.; Yamato, M.; Hirose, M.; Takahashi, C.; Isoi, Y.; Kikuchi, A.; Okano, T. Novel Approach for Achieving Double-Layered Cell Sheets Co-Culture: Overlaying Endothelial Cell Sheets onto Monolayer Hepatocytes Utilizing Temperature-Responsive Culture Dishes. *J. Biomed. Mater. Res.* **2002**, *62*, 464–470.
22. Arshady, R.; Corain, B.; Zecca, M.; Jayakrishnan, A.; Horak, D. Amphiphilic Functional Microgels. *Microspheres, Microcapsules Liposomes* **2002**, *4*, 203–251.
23. Song, L.; Liang, D.; Fang, D.; Chu, B. Fast DNA Sequencing up to 1000 Bases by Capillary Electrophoresis Using Poly(N,N-Dimethylacrylamide) as a Separation Medium. *Electrophoresis* **2001**, *22*, 1987–1996.
24. Horbett, T. A.; Brash, J. L. Proteins at Interfaces: Current Issues and Future Prospects. *ACS Symp. Ser.* **1987**, *343*, 1–33.
25. Brash, J. L.; Horbett, T. A. Proteins at Interfaces. An Overview. *ACS Symp. Ser.* **1995**, *602*, 1–23.
26. Saito, N.; Matsuda, T. Protein Adsorption on Self-Assembled Monolayers with Water-Soluble Non-Ionic Oligomers Using Quartz-Crystal Microbalance. *Mater. Sci. Eng., C: Biomimetic Mater., Sens. Syst.* **1998**, *C6*, 261–266.
27. Benoit, D.; Chaplinski, V.; Braslau, R.; Hawker, C. J. Development of a Universal Alkoxyamine for "Living" Free Radical Polymerizations. *J. Am. Chem. Soc.* **1999**, *121*, 3904–3920.
28. Gotz, H.; Harth, E.; Schiller, S. M.; Frank, C. W.; Knoll, W.; Hawker, C. J. Synthesis of Lipo-Glycopolymer Amphiphiles by Nitroxide-Mediated Living Free-Radical Polymerization. *J. Polym. Sci, Part A, Polym. Chem.* **2002**, *40*, 3379–3391.
29. Schierholz, K.; Givehchi, M.; Fabre, P.; Nallet, F.; Papon, E.; Guerret, O.; Gnanou, Y. Acrylamide-Based Amphiphilic Block Copolymers via Nitroxide-Mediated Radical Polymerization. *Macromolecules* **2003**, *36*, 5995–5999.
30. Bosman, A. W.; Vestberg, R.; Heumann, A.; Frechet, J. M. J.; Hawker, C. J. A Modular Approach toward Functionalized Three-Dimensional Macromolecules: From Synthetic Concepts to Practical Applications. *J. Am. Chem. Soc.* **2003**, *125*, 715–728.
31. Rademacher, J. T.; Baum, M.; Pallack, M. E.; Brittain, W. J.; Simonsick, W. J., Jr. Atom Transfer Radical Polymerization of N,N-Dimethylacrylamide. *Macromolecules* **2000**, *33*, 284–288.
32. Lutz, J.-F.; Neugebauer, D.; Matyjaszewski, K. Stereoblock Copolymers and Tacticity Control in Controlled/Living Radical Polymerization. *J. Am. Chem. Soc.* **2003**, *125*, 6986–6993.
33. Kizhakkedathu, J. N.; Brooks, D. E. Synthesis of Poly(N,N-Dimethylacrylamide) Brushes from Charged Polymeric Surfaces by Aqueous ATRP: Effect of Surface Initiator Concentration. *Macromolecules* **2003**, *36*, 591–598.
34. Neugebauer, D.; Matyjaszewski, K. Copolymerization of N,N-Dimethylacrylamide with N-Butyl Acrylate *via* Atom Transfer Radical Polymerization. *Macromolecules* **2003**, *36*, 2598–2603.
35. Donovan, M. S.; Lowe, A. B.; Sumerlin, B. S.; Mccormick, C. L. RAFT Polymerization of N,N-Dimethylacrylamide Utilizing Novel Chain Transfer Agents Tailored for High Reinitiation Efficiency and Structural Control. *Macromolecules* **2002**, *35*, 4123–4132.
36. Donovan, M. S.; Sanford, T. A.; Lowe, A. B.; Sumerlin, B. S.; Mitsukami, Y.; Mccormick, C. L. RAFT Polymerization of N,N-Dimethylacrylamide in Water. *Macromolecules* **2002**, *35*, 4570–4572.

37. Boyes, S. G.; Brittain, W. J.; Weng, X.; Cheng, S. Z. D. Synthesis, Characterization, And Properties of ABA Type Triblock Copolymer Brushes of Styrene and Methyl Acrylate Prepared by Atom Transfer Radical Polymerization. *Macromolecules* **2002**, *35*, 4960–4967.
38. Beinhoff, M.; Appapillai, A. T.; Underwood, L. D.; Frommer, J. E.; Carter, K. R. Patterned Polyfluorene Surfaces by Functionalization of Nanoimprinted Polymeric Features. *Langmuir* **2006**, *22*, 2411–2414.
39. Green, N. M. Avidin and Streptavidin. *Methods Enzymol.* **1990**, *184*, 51–67.
40. Wilchek, M.; Bayer, E. A. Introduction to Avidin-Biotin Technology. *Methods Enzymol.* **1990**, *184*, 5–13.
41. Salem, A. K.; Rose, F. R. A. J.; Oreffo, R. O. C.; Yang, X.; Davies, M. C.; Mitchell, J. R.; Roberts, C. J.; Stolnik-Trenkic, S.; Tendler, S. J. B.; Williams, P. M.; Shakesheff, K. M. Porous Polymer and Cell Composites that Self-Assemble in Situ. *Adv. Mater.* **2003**, *15*, 210–213.
42. Lee, K.-B.; Yoon, K. R.; Woo, S. I.; Choi, I. S. Surface Modification of Poly(Glycolic Acid) (PGA) for Biomedical Applications. *J. Pharmaceut. Sci.* **2003**, *92*, 933–937.
43. Hong, M.-Y.; Yoon, H. C.; Kim, H.-S. Protein-Ligand Interactions at Poly(Amidoamine) Dendrimer Monolayers on Gold. *Langmuir* **2003**, *19*, 416–421.
44. Sun, X.-L.; Faucher, K. M.; Houston, M.; Grande, D.; Chaikof, E. L. Design and Synthesis of Biotin Chain-Terminated Glycopolymers for Surface Glycoengineering. *J. Am. Chem. Soc.* **2002**, *124*, 7258–7259.
45. Nishida, J.; Nishikawa, K.; Nishimura, S.-I.; Wada, S.; Karino, T.; Nishikawa, T.; Ijiro, K.; Shimomura, M. Preparation of Self-Organized Micro-Patterned Polymer Films Having Cell Adhesive Ligands. *Polym. J.* **2002**, *34*, 166–174.
46. Lahann, J.; Balcells, M.; Lu, H.; Rodon, T.; Jensen, K. F.; Langer, R. Reactive Polymer Coatings: A First Step toward Surface Engineering of Microfluidic Devices. *Anal. Chem.* **2003**, *75*, 2117–2122.
47. Hyun, J.; Zhu, Y.; Liebmann-Vinson, A.; Beebe, T. P., Jr.; Chilkoti, A. Microstamping on an Activated Polymer Surfaces: Patterning Biotin and Streptavidin onto Common Polymeric Biomaterials. *Langmuir* **2001**, *17*, 6358–6367.
48. Shim, M.; Kam, N. W. S.; Chen, R. J.; Li, Y.; Dai, H. Functionalization of Carbon Nanotubes for Biocompatibility and Biomolecular Recognition. *Nano Lett.* **2002**, *2*, 285–288.
49. Faucher, K. M.; Sun, X.-L.; Chaikof, E. L. Fabrication and Characterization of Glycocalyx-Mimetic Surfaces. *Langmuir* **2003**, *19*, 1664–1670.
50. Lahann, J.; Balcells, M.; Rodon, T.; Lee, J.; Choi, I. S.; Jensen, K. F.; Langer, R. Reactive Polymer Coatings: A Platform for Patterning Proteins and Mammalian Cells onto a Broad Range of Materials. *Langmuir* **2002**, *18*, 3632–3638.
51. Hyun, J.; Chilkoti, A. Micropatterning Biological Molecules on a Polymer Surface Using Elastomeric Microwells. *J. Am. Chem. Soc.* **2001**, *123*, 6943–6944.
52. Um, S. H.; Lee, G. S.; Lee, Y.-J.; Koo, K.-K.; Lee, C.; Yoon, K. B. Self-Assembly of Avidin and D-Biotin-Tethering Zeolite Microcrystals into Fibrous Aggregates. *Langmuir* **2002**, *18*, 4455–4459.